Desalination and Water Treatment
www.deswater.com

doi: 10.1080/19443994.2013.815682

52 (2014) 5333–5342
August

Taylor & Francis
Taylor & Francis Group

Modelling ion exchange kinetics in zeolyte-type materials using Maxwell-Stefan approach

Patrícia Ferreira Lito, José Pedro Salgado Aniceto, Carlos Manuel Silva*

Department of Chemistry, CICECO, University of Aveiro, Campus Universitário de Santiago, Aveiro 3810-193, Portugal
Tel. +351 234 401549; Fax: +351 234 370084; email: carlos.manuel@ua.pt

Received 21 August 2012; Accepted 16 May 2013

ABSTRACT

In this essay, the Maxwell-Stefan (MS) formalism was adopted to model the removal of cadmium(II) and mercury(II) ions from aqueous solutions using microporous titanosilicate ETS-4. The embodied transport mechanism is surface diffusion, since the small pore diameters of such zeolite-type materials imply that counter ions never escape from the force field of the matrix co-ions, mainly owing to the strong and long range electrostatic interactions. The parameters of the global model are the MS diffusivities of ion–ion and ion–solid pairs, and a convective mass transfer coefficient. The average absolute relative deviations (AARD) achieved for Cd^{2+}/Na^{+}/ETS-4 and Hg^{2+}/Na^{+}/ETS-4 systems were only 3.47 and 7.34%, respectively. The model calculates concentration profiles and their evolution along time under transient regime, being able to represent the initial steep branches of removal curves and subsequent transition to equilibrium, where kinetic curves are frequently very difficult to fit. The well-known and frequently used pseudo-first and pseudo-second-order equations were also chosen for comparison, and provided large deviations: AARD(Cd^{2+}) = 48.9% and AARD(Hg^{2+}) = 26.6 % (first order), and AARD(Cd^{2+}) = 29.0% and AARD(Hg^{2+}) = 54.6% (second order).

Keywords: Ion exchange; Kinetics; Modelling; Maxwell-Stefan; Diffusion; Titanosilicate

1. Introduction

Modelling and simulation are fundamental tools in the prediction of the dynamic and equilibrium behaviour, optimisation of operating conditions and scaling up of chemical plants. Ion exchange is one of the most effective and commonly applied methods to uptake ionic contaminants from waters and wastewaters, and recovers valuable metals [1–3]. With respect to equilibrium, the most important and theoretically sound models have been reviewed in detail elsewhere [4]. Summarily, they can be divided into four groups: homogeneous mass action models, heterogeneous adsorption models, heterogeneous mass action models and purely empirical models [5–12]. In regard to ion exchange kinetics, it is controlled by diffusion of the ions either inside the exchanger or in the film surrounding the particle. The existing rate models correctly represent the external diffusion through the film [13,14], but the description of the intraparticle diffusion is by far more complex considering the interactions between ions, co-ions and solid matrix [4]. The exchanger phase influences decisively mass

*Corresponding author.

transfer not only due to the kind and abundance of fixed ionic charges, but also due to their spatial distribution and to the pore size distribution of the solid, which ultimately determines the intraparticle transport mechanisms and so the effective diffusivities of the participant species.

The ion exchange kinetics is frequently represented in the literature by semi-empirical pseudo-first and pseudo-second-order equations [15–17], though they possess no strict theoretical background and, consequently, have restricted application and extrapolation capability [4]. Instead, the Nernst-Planck equations are physically supported and have been successfully applied to describe mass transport in dilute ionic systems [4,18]. These equations take into account the electric field generated as a result of the distinct mobilities of counter ions. When the electrochemical gradients are neglected, the flux of exchangeable ions through the pellet can be described by Fick's first law [4,19,20], for which numerous solutions were obtained for a variety of initial and boundary conditions, giving rise to several single-particle methods frequently used to evaluate the implied diffusion coefficients [4]. An alternative approach concerns the application of the Maxwell-Stefan (MS) equations, due to their well-documented advantages in mass transfer: (1) they take into account and distinguish both ion–ion and ion–solid interactions; (2) one diffusivity coefficient is defined for each pair of components, being dependent on their properties only; (3) the coefficients are weakly dependent on composition; (4) the equations are particularly advantageous at high concentrations; and (5) they are applicable and easily extended to multi-component systems [4,18]. Beyond their original application in non-ionic systems, the MS equations were applied to resins [21,22] and found recent relevance for electrolyte mixtures in membrane electrolysis (e.g. [23,24]) and electrodialysis [25].

In this work, the MS formalism is adopted to model the removal of cadmium(II) and mercury(II) ions from aqueous solutions using microporous titanosilicate ETS-4. In the modelling section below, it is shown that the ionic transport mechanism in ETS-4 is surface diffusion. The MS equations are adapted and proposed with advantage to describe the rate of ion exchange in such microporous materials.

Titanosilicates are zeolite-type materials which have attracted increasingly attention because of their high stability, ion exchange properties and selectivity. They are formed by a three-dimensional combination of tetrahedral and octahedral building blocks carrying a -2 global charge neutralised by extra-framework exchangeable cations which confer them a high cation exchange capacity [26]. For example, ETS-10 has been shown to have high selectivity for toxic metals like Pb^{2+}, Cu^{2+}, Cd^{2+}, Co^{2+}, Mn^{2+}, Zn^{2+}, Cs^{+}, Ag^{+}, Tl^{+}, Sr^{2+}, Hg^{2+}, Sb^{3+} and Th^{4+} [2,27–31]. Lopes et al. [32–35] evaluated the potential of synthetic microporous (ETS-4, ETS-10 and AM-2) and layered (AM-4) titanosilicates for decontamination of natural waters polluted with low mercury levels and found they have a great potential for wastewater purification. Barreira et al. [36] and Ferreira et al. [37] investigated the capacity of ETS-4 for cadmium(II) uptake. Both studies revealed the large ion exchange capacity of ETS-4 and their high removal efficiencies. Later, Otero et al. [38] published the removal of Hg^{2+} and Cd^{2+} with ETS-4, being possible to observe the high selectivity of titanosilicate for both toxic metal ions. Recently, Cardoso et al. studied the competitive removal of Hg^{2+} and Cd^{2+} with ETS-4 and measured the kinetic and equilibrium selectivities of the separation [39].

The potential of these small pore zeolite-type materials leads us to study the ion exchange kinetics of systems where they are most promising and effective. Accordingly, in the following section, we develop the MS based model and present the numerical solution approach. Due to their expressive application, the pseudo-first and pseudo-second-order equations were adopted for comparison. After that, the data used in calculations are discussed, along with their experimental conditions. Then, the modelling results are presented and analysed in detail, and the most important conclusions are drawn at the end.

2. Modelling

In this section, the MS based model developed to represent the experimental data is firstly described. The MS equations are manipulated and applied to ion exchange, and then the material balances, initial and boundary conditions, and equilibrium isotherms are presented, as well as the numerical solution approach. In the last part, the pseudo-first and pseudo-second-order rate equations adopted for comparison are summarily presented.

2.1. Maxwell-Stefan (MS) based model

2.1.1. Maxwell-Stefan equations

Ion exchange between counter ions A^{z_A} and B^{z_B} can be represented by a conventional chemical equilibrium which for a solid and solution initially in B and A forms, respectively, is written as:

$$z_A\overline{B^{z_B}} + z_B A^{z_A} \leftrightarrow z_B\overline{A^{z_A}} + z_A B^{z_B} \quad (1)$$

where z_A and z_B are the electrochemical valences, and the upper bars identify the solid phase. In this essay, the exchanger is ETS-4, counter ion A^{z_A} is Na^+, and B^{z_B} is Cd^{2+} or Hg^{2+}. The crystalline nature of titanosilicate means it possesses a uniform distribution of fixed ionic charges (co-ions). Moreover, its small micropores implies that both counter ions never escape from the force field of the matrix co-ions, mainly owing the strong and long range nature of the electrostatic interactions. Accordingly, surface diffusion is the mass transport mechanism of counter ions inside titanosilicate.

Analogously to the dusty gas model [40,41], the counter ions are the components $1,\ldots,n$, and the fixed ionic charges of the titanosilicate are the $(n+1)$th component (with null velocity, $u_{n+1}=0$). Accordingly, the MS transport equation of species i in multicomponent isothermal ionic systems is:

$$-\nabla\mu_i - Fz_i\nabla\phi = \sum_{\substack{j=1\\ j\neq i}}^{n} \frac{y_j\Re T(u_i-u_j)}{\bar{D}_{ij}} + \frac{y_s\Re T u_i}{\bar{D}_{is}} \tag{2}$$

where $\nabla\mu_i$ is the chemical potential gradient of i, z_i is the charge of component i, $\bar{D}_{ij}$ is the MS diffusivity of pair $i-j$, $\bar{D}_{is}$ is the MS diffusivity corresponding to the interaction between i and the fixed ionic charges (subscript s stands for solid), $y_j = q_j/q_t$ is the molar fraction of counter ion j in the solid, $y_s = Q/q_t$ is the molar fraction of fixed charged groups, q_j is the molar concentration of j in the solid, q_t is the total concentration of ionic species in the solid, u_j is the intraparticle velocity of j, F is Faraday constant, $\Re$ is gas constant, T is absolute temperature and finally, ϕ is the electrostatic potential. It should be noted that $\sum_{i=1}^{n+1} y_i = 1$, and q_t is constant when counter ions have equal valences. Taking into account the definition of molar flux, $N_j = q_t y_j u_j$, Eq. (2) may be recast as:

$$-\frac{y_i}{\Re T}\nabla\mu_i - y_i z_i \frac{F}{\Re T}\nabla\Phi = \sum_{\substack{j=1\\ j\neq i}}^{n} \frac{y_j N_i - y_i N_j}{q_t \bar{D}_{ij}} + \frac{y_s N_i}{q_t \bar{D}_{is}} \tag{3}$$

Assuming equilibrium between exchanger and a hypothetical solution of concentration x_i^*, one can write $\mu_i = \mu_{i,eq.sol}$. Hence, $\nabla\mu_i$ can be computed in terms of the molar fraction gradients of counter ions in the solid by:

$$\frac{y_i}{\Re T}\nabla\mu_i = \sum_{j=1}^{n} \Gamma_{ij}\nabla y_j, \text{ with } \Gamma_{ij} \equiv y_i \frac{\partial Ln(\gamma_{i,eq.sol}x_{i,e})}{\partial y_j} \tag{4}$$

where $\gamma_{i,eq.sol}$ is the activity coefficient of counter ion i in solution under equilibrium, Γ_{ij} is thermodynamic factor, $x_i = C_i/C_t$ and C_i are molar fraction and concentration of i in solution, C_t is total concentration of ionic species in bulk solution and $x_{i,e}$ and y_i are related by the equilibrium isotherm of the system. In n-dimensional matrix notation, Eq. (3) becomes:

$$(N) = -q_t[B]^{-1}[\Gamma](\nabla y) - q_t[B]^{-1}(\nabla\xi) \tag{5}$$

where (N) is the vector of molar fluxes, (∇y) is the vector containing the gradients of counter ions, $[\Gamma]$ is the matrix of thermodynamic factors and the elements of matrix $[B]$ and vector $(\nabla\xi)$ are defined as:

$$B_{ii} = \frac{y_s}{\bar{D}_{is}} + \sum_{\substack{j=1\\ j\neq i}}^{n} \frac{y_j}{\bar{D}_{ij}}, \quad B_{ij} = -\frac{y_i}{\bar{D}_{ij}} \tag{6}$$

$$\nabla\xi_i = y_i z_i \frac{F}{\Re T}\nabla\phi \tag{7}$$

The electroneutrality and nonexistent electric current inside exchanger implies that $\sum_{i=1}^{n+1} q_i z_i = 0$ and $\sum_{i=1}^{n+1} z_i N_i = 0$, which can be combined to eliminate $\nabla\phi$ from the generalised MS equations, since the following relation is adhered to:

$$\frac{F}{\Re T}\nabla\phi = \frac{-\sum_{i=1}^{n} z_i \left(\sum_{j=1}^{n} L_{ij}\nabla y_j\right)}{\sum_{i=1}^{n} y_i z_i \left(\sum_{i=1}^{n} z_j L_{ji}\right)}, \text{ where } [L] = [B]^{-1} \tag{8}$$

2.1.2. Material balances, initial and boundary conditions and equilibrium isotherms

The material balances to the spherical exchanger particle and to the stirred reservoir are:

$$\left(\frac{\partial q_A}{\partial t}\right) = -\frac{1}{r^2}\frac{\partial}{\partial r}(r^2 N_A) \tag{9}$$

$$\frac{d\,C_A}{dt} = -\frac{V_s}{V_L}\frac{d\,\bar{q}_A}{dt} \tag{10}$$

$$\bar{q}_A = \frac{3}{R^3}\int_0^R r^2 q_A\, dr \tag{11}$$

where $\bar{q}_A$ is the average loading per unit particle volume, R is the particle radius, V_s is the volume of exchanger and V_L is the volume of fluid phase. The initial (no B in solution, no A in solid) and boundary conditions, and the restriction of continuity of fluxes at particle surface are:

$$t = 0,\ \begin{cases} q_A = \bar{q}_A = 0 \\ C_A = C_{A,0} \end{cases} \tag{12}$$

$$r = R,\ q_A = q_{A,R} \tag{13}$$

$$r = 0,\ \left(\frac{\partial q_A}{\partial r}\right) = 0 \tag{14}$$

$$N_A|_{r=R} = k_f(C_A - C_{A,R}) \tag{15}$$

The equilibrium between bulk solution and exchanger phase (titanosilicate) for the systems under study in this work is given by the Langmuir (L) isotherm, which involves parameters $q_{\max}$ and K_L:

$$q_A = \frac{q_{\max}\, K_L\, C_A}{1 + K_L\, C_A} \tag{16}$$

2.1.3. Numerical solution

The MS model listed above was solved numerically using the Method of Lines [42] and integrated by the finite-difference approach with central differences of second order. Forward and backward differences formulas were adopted for the first and last nodes, respectively. The average loading per unit particle volume (Eq. (11)) was numerically evaluated using the 1/3 Simpson's Rule. The MS diffusivities and the convective mass transfer coefficient are the model parameters to fit to the experimental data.

2.2. Pseudo-first and pseudo-second-order models

The pseudo-first-order rate equation of Lagergren is one of the most widely used to represent the ion exchange process. It is represented by:

$$\frac{d\bar{q}_A}{dt} = k_1\ (\bar{q}_{A,e} - \bar{q}_A) \tag{17}$$

where k_1 is the rate constant of the first-order equation and $\bar{q}_{A,e}$ is the sorbed cation concentration at equilibrium. The top bars denote average concentrations. After partial integration, from $t = 0$ and $\bar{q}_A = 0$, one obtains:

$$\mathrm{Ln}(\bar{q}_{A,e} - \bar{q}_i) = \mathrm{Ln}(\bar{q}_{A,e}) - k_1\ t \tag{18}$$

from which k_1 can be determined when experimental data is available. The unknown values of $\bar{q}_{A,e}$ can be calculated from the isotherm combined with trivial material balance.

The pseudo-second-order rate equation is also based on the sorption capacity of the solid and possesses one constant, k_2, that can be fitted to experimental data. Its differential and integrated forms are:

$$\frac{d\bar{q}_A}{dt} = k_2(\bar{q}_{A,e} - \bar{q}_A)^2 \tag{19}$$

$$\frac{t}{q_A} = \frac{1}{k_2\bar{q}_{A,e}^2} + \frac{1}{\bar{q}_{A,e}}t \tag{20}$$

It is worth noting that both k_1 and k_2 depend on the relative amounts of solid and fluid in the experiments used to extract them. This prevents their further use to simulate any other units, namely open systems or even closed systems under distinct conditions. In this context, these models are useless.

3. Ion exchange data

The data used in the calculations refer to batch experiments, where cadmium(II) and mercury(II) are removed from aqueous solutions using ETS-4 initially in Na-form (data from Otero et al. [38]). The experiments were carried out at fixed temperature, pH, volume of solution and initial solution concentration (except one point) using different titanosilicate masses. There are three removal curves for each system, Hg^{2+}/Na^+/ETS-4 and Hg^{2+}/Na^+/ETS-4. In Table 1, the conditions of these experiments are listed, and the relevant features of ETS-4 are compiled in Table 2. In the following, subscripts A denote Hg^{2+} or Cd^{2+}, and subscript B symbolises Na^+. The isotherms of the previous systems are:

$$q_{Hg^{2+}} = \frac{0.43 \times 34.14\ \times 10^{-3} C_{Hg^{2+}}}{1 + 34.14\ \times 10^{-3} C_{Hg^{2+}}} \quad \text{and} \quad q_{Cd^{2+}} = \frac{0.24 \times 7.46\ \times 10^{-3} C_{Cd^{2+}}}{1 + 7.46\ \times 10^{-3} C_{Cd^{2+}}} \tag{21}$$

when q_A is expressed in $\mathrm{molkg}^{-1}$and C_A in molm^{-3}.

Table 1
Experimental conditions of the data used in calculations for Cd^{2+} and Hg^{2+} removal using ETS-4: mass of ETS-4, initial concentration of cation solution, initial ratio of cation moles to ETS-4 mass. Fixed variables: $T = 295 \pm 1$ K, $V_L = 2 \times 10^{-3} m^3$, pH = 4 [38]

System	Variable	Exp. 1	Exp. 2	Exp. 3
Hg^{2+}/Na^+/ ETS-4	$m_{ETS\text{-}4}$ (mg)	1.639	2.223	5.055
	$C_{A,0}(10^{-6}$kg m$^{-3})$	50	50	50
	$(n_A/m_{ETS\text{-}4})_0$(mol kg^{-1})	0.30	0.22	0.10
Cd^{2+}/Na^+/ ETS-4	$m_{ETS\text{-}4}$ (mg)	50.5	50.4	100.2
	$C_{A,0}(10^{-6}$kg m$^{-3})$	0.84	0.64	0.62
	$(n_A/m_{ETS\text{-}4})_0$(mol kg^{-1})	0.30	0.23	0.11

Table 2
Features of titanosilicate ETS-4 particles used [43]

Formula	$[Na_9Ti_5Si_{12}O_{38}(OH).12H_2O]$
Density, kg m^{-3}	2,200
Ion exchanger capacity, eq kg^{-1}	6.39
Particle diameter, 10^{-6}m	0.5–0.9
Pore diameter, 10^{-10}m	3–4

4. Results and discussion

This section starts with a brief discussion of the experimental curves selected for modelling. Then, the calculated results are presented and analysed in detail. The correlated kinetic curves and the predicted concentration profiles inside the particle are given and discussed individually. Finally, the predictive capability of the model under research is evaluated.

4.1. Trends of the experimental kinetic curves

In Fig. 1(a) and (b), the evolution of the concentrations of cadmium(II) and mercury(II), respectively, along time are shown. The trends are very similar in both systems. The solid load begins in zero, since ETS-4 is initially in Na-form, and then increases towards the equilibrium where q_A remains constant. In the case of Hg^{2+}, one of the curves does not attain equilibrium, as the horizontal plateau is absent. In terms of velocity, all curves exhibit a fast initial metal uptake, followed by the characteristic slower removal approaching equilibrium, due to the large driving force for ion transport at the beginning of the process.

It is worth noting that there is a correspondence between both sets of experiments, taking account of the very near ratios between the molar quantity of cation and mass of titanosilicate: 0.1, 0.22 and 0.30 mol kg^{-1}for Hg^{2+}/Na^+/ETS-4, and 0.11, 0.23 and 0.30 mol kg^{-1}for Cd^{2+}/Na^+/ETS-4 (see Table 1). Since the solution volume is fixed (2 L), it is possible to conclude that Hg^{2+} is sorbed more slowly than Cd^{2+} at the working temperature. In fact, under these experimental conditions, 48 h are sufficient for the cadmium (II) systems equilibration, while 72 h are not enough for mercury(II) at 0.30 and 0.22 mol kg^1. It will be shown next that the MS diffusion coefficients corroborate these observations.

4.2. Calculated results and modelled kinetic curves

The uptake curves calculated by the MS based model are plotted against time in Fig. 1(a) and (b),

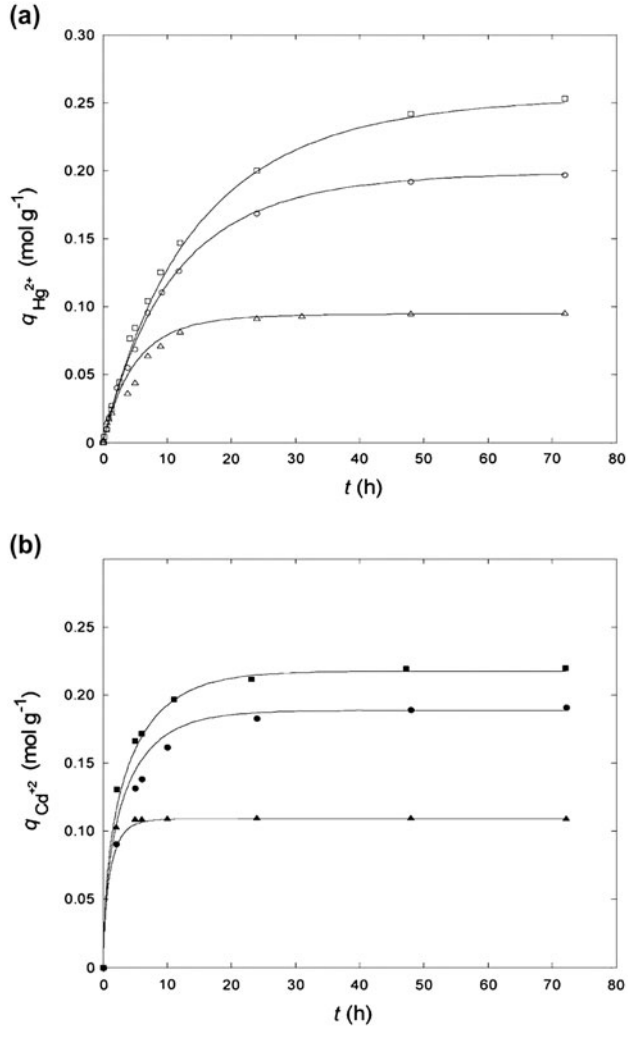

Fig. 1. Experimental and calculated concentrations of sorbed metal vs. time for the (a) Hg^{2+}/Na^+/ETS-4 system and (b) Cd^{2+}/Na^+/ETS-4 system. Lines: MS based model of this work. Data: experimental conditions in Table 1: □ and ■, Exp.1; ○ and ●, Exp.2; Δ and ▲, Exp.3.

along with experimental data. The optimised parameters, namely the MS diffusivities and convective mass transfer coefficients, are listed together with the corresponding average absolute relative deviations (AARD) in Table 3. Both figures exhibit excellent agreement between model results and experimental data, which is confirmed by the low deviations found: AARD = 7.34% for Hg^{2+}/Na^{+}/ETS-4 and AARD = 3.47% for Cd^{2+}/Na^{+}/ETS-4. The MS based model is able to represent the data very well, even the initial steep ascent branches and their transition to equilibrium, where kinetic curves are frequently very difficult to fit. Only the mercury(II) curve corresponding to $(n_{Hg^{2+}}/m_{ETS\text{-}4})_0 = 0.10\ mol\ kg^{-1}$ deviates slightly more (10.9%), causing the global AARD to reach 7.34%.

The MS diffusivities $Đ_{AS}$ and $Đ_{AB}$ are smaller in the case of Hg^{2+}/Na^{+}/ETS-4 system: 2.398×10^{-18} and 6.471×10^{-20} m^2s^{-1} in opposition to 2.776×10^{-18} and 2.568×10^{-19} m^2s^{-1} found for Cd^{2+}/Na^{+}/ETS-4 (see Table 3). These values justify the dissimilar kinetic behaviours discussed above, as the inferior transport coefficients of mercury(II) give undoubtedly rise to slower ion exchange kinetics. It is interesting to check that these results are in accordance with the effective ionic radius of both species: 102 pm for Hg^{2+} and only 95 pm for Cd^{2+} [44]. Taking into account they possess the same charge (+2), the larger cation will have more limited diffusivity in the same solid matrix. With respect to the sodium cation, the MS diffusivities optimised from the two independent sets of experiments are similar, which is a good finding since they refer to the same exchanger material (1.785×10^{-18} and 1.690×10^{-18} m^2s^{-1}). Before concluding this part of the discussion, it is important to refer that in the literature very small diffusivities are usually found for ions inside microporous materials, as, for instance, 1.14×10^{-17} (Na^+), 1.96×10^{-21} (K^+) and 8.27×10^{-26} (Rb^+) in Analcite [45]; 10^{-18}–10^{-19} (Na^+/K^+) in Chabazite [46]; 2.00×10^{-18} ($2Na^+ \rightarrow Ca^{2+}$) and 6.53×10^{-18} ($2Na^+ \rightarrow Mg^{2+}$) in Beryllophosphate-G [47]; 1.8×10^{-17} ($Ca^{2+} \rightarrow Na^+$) and 8.0×10^{-18} ($Mg^{2+} \rightarrow Na^+$) in Zeolite-NaA (semi-crystallyne) [48] and 1.082×10^{-15} (Cd^{2+}), 2.319×10^{-15} (Na^+) in ETS-10 [29].

The normalised concentrations of Hg^{2+} in the ETS-4 are plotted against time in Fig. 2 for three different particle positions: at surface ($r = R$), half radius ($r = R/2$) and centre ($r = 0$). The reduction was performed with the final equilibrium metal loading, $q_{A,e}$ and the curves were calculated with the MS based model for the experimental conditions Exp. 3 of Table 1. The three functions are denoted by $q_{A,r}(t)/q_{A,e}$, where

Table 3
Calculated results obtained with the MS based model of this work, and with the pseudo-first and pseudo-second-order correlations adopted for comparison (Consult experimental condition in Table 1)

Maxwell-Stefan based model results

System	$Đ_{As}$, (m^2s^{-1})	$Đ_{Bs}$ (m^2s^{-1})	$Đ_{AB}$ (m^2s^{-1})	k_f ($m\ s^{-1}$)	AARD(%)
Hg^{2+}/Na^{+}/ETS-4	2.398×10^{-18}	1.785×10^{-18}	6.471×10^{-20}	5.719×10^{-6}	7.34
Cd^{2+}/Na^{+}/ETS-4	2.776×10^{-18}	1.690×10^{-18}	2.568×10^{-19}	2.092×10^{-6}	3.47

Pseudo-first-order model results

(Global deviations : $AARD_{Cd^{2+}} = 48.9\%$ and $AARD_{Hg^{2+}} = 26.6\%$); $k_1(h^{-1})$ and AARD(%)

System	Exp. 1	Exp. 2	Exp. 3
Hg^{2+}/Na^{+}/ETS-4	$k_1 = 0.07231$	$k_1 = 0.04445$	$k_1 = 0.05435$
	AARD = 6.9	AARD = 32.3	AARD = 39.6
Cd^{2+}/Na^{+}/ETS-4	$k_1 = 0.06978$	$k_1 = 0.04491$	$k_1 = 0.008751$
	AARD = 31.0	AARD = 37.3	AARD = 78.4

Pseudo-second-order model results

(Global deviations : $AARD_{Cd^{2+}} = 29.0\%$ and $AARD_{Hg^{2+}} = 54.6\%$); $k_2(kgmol^{-1}h^{-1})$ and AARD(%)

System	*Exp. 1*	*Exp. 2*	Exp. 3
Hg^{2+}/Na^{+}/ETS-4	$k_2 = 1.231$	$k_2 = 1.088$	$k_2 = 1.017$
	AARD = 88.1	AARD = 49.1	AARD = 28.5
Cd^{2+}/Na^{+}/ETS-4	$k_2 = 1.005$	$k_2 = 0.9479$	$k_2 = 1.650$
	AARD = 17.1	AARD = 12.0	AARD = 57.8

$r = 0,\ R/2,\ R$. Similar trends were obtained for the remaining conditions of Hg^{2+}/Na^{+}/ETS-4, and for the three experiments of the cadmium(II) system.

The normalised concentration at surface evidences an interesting behaviour that deserves special commentary. The initial sudden increase of $q_{A,R}(t)/q_{A,e}$ is so pronounced that it passes through a maximum (even higher than 1.0) and then decreases gradually until the equilibrium. Without external mass transfer resistance, the initial particle concentration at surface would suddenly increase from $q_{A,R}(t = 0^{-}) = 0$ to $q_{A,R}(t = 0^{+}) = q_{A,e}(C_{A0})$, which is the solid concentration in equilibrium with bulk solution. Then, $q_{A,R}(t)$ would decrease monotonously until the final equilibrium is reached, i.e. $q_{A,R}(t) \rightarrow q_{A,e} = q_{A,R}(t = \infty)$. However, the existence of the film diffusion smoothes this initial step increase, as Fig. 2 illustrates.

In contrast, inside the particle and far from surface the concentration increases monotonously as both $q_{A,R/2}(t)/q_{A,e}$ and $q_{A,0}(t)/q_{A,e}$ point out in Fig. 2. These functions have the same boundary values (start at 0.0 and end at 1.0), but inside the interval $q_{A,0}(t)/q_{A,e}$ is smaller than $q_{A,0}(t)/q_{A,e}$ since the diffusion path to the particle centre is the highest one. This fact delays the increasing of the concentration.

The results obtained with the pseudo-first and pseudo-second-order correlations adopted for comparison are listed in Table 3. In the whole, both expressions provide very inaccurate results, as the global deviations accomplished by the pseudo-first-order equations are $AARD_{Cd^{2+}} = 48.9\%$ and $AARD_{Hg^{2+}} = 26.6\%$, and by the pseudo-second-order equations are $AARD_{Cd^{2+}} = 29.0\%$

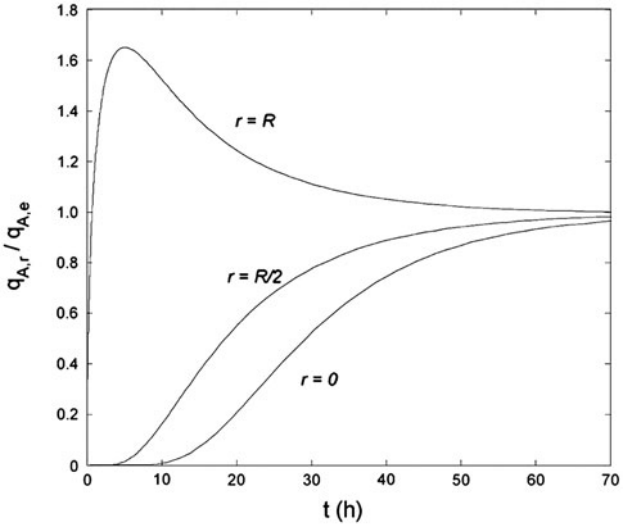

Fig. 2. Normalised concentration of Hg^{2+} against time at the surface, half radius, and centre of the ETS-4 particle. Calculations accomplished with MS based model of this work for Exp. 3 (see Table 1).

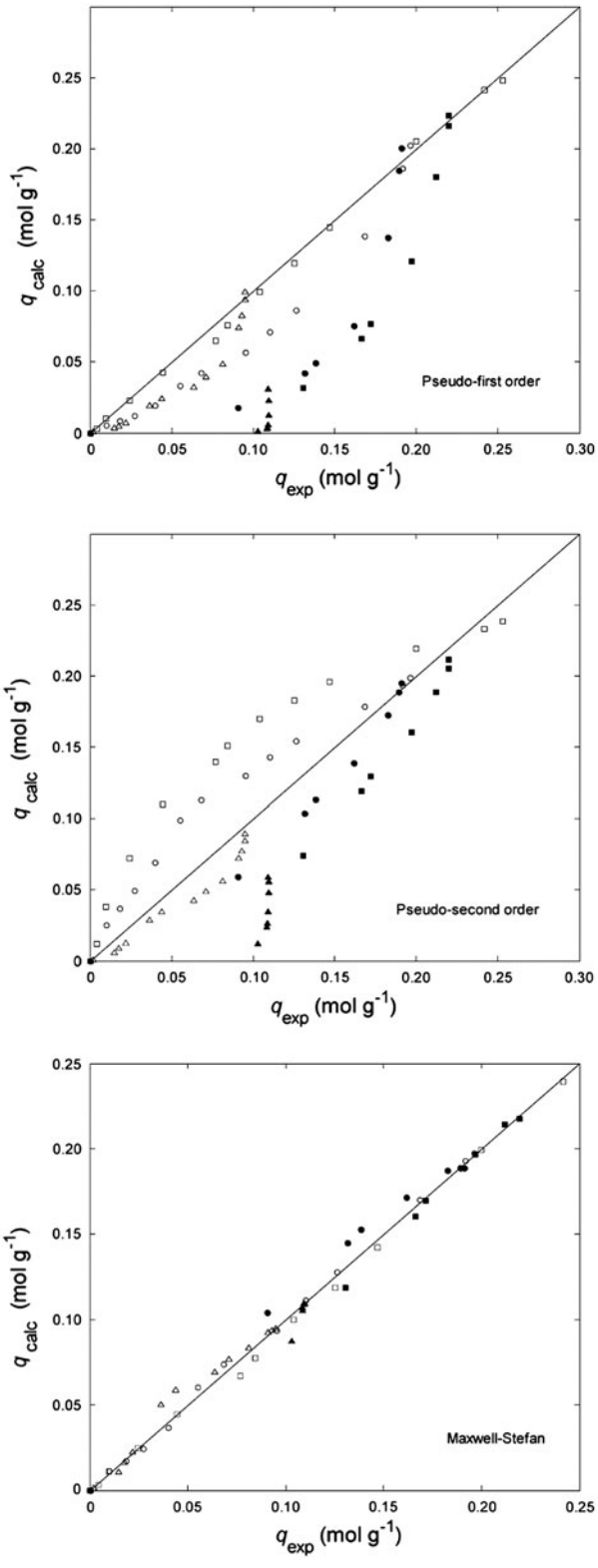

Fig. 3. Comparison between calculated and experimental Cd^{2+} (black symbols) and Hg^{2+} (white symbols) concentrations in the ETS-4. Models: MS, pseudo-first-order, and pseudo-second-order. Data: experimental conditions in Table 1: □ and ■, Exp.1; ○ and ●, Exp.2; Δ and ▲, Exp. 3.

and $AARD_{Hg^{2+}} = 54.6\%$. It is worth noting that these equations fit one parameter per curve which means that each of the previous global deviations involves three constants, k_1 or k_2. On the other hand, the MS based model achieves only $AARD_{Hg^{2+}} = 7.34\%$ and $AARD_{Cd^{2+}} = 3.47\%$, which are very small values even taking into account it embodies one additional parameter (i.e. four totally). In Fig. 3, the calculated vs. experimental $\bar{q}_A$values are plotted and evidence the following points: (1) the poor performance of the pseudo-first and pseudo-second-order equations in contrast to the good behaviour provided by the MS based model; (2) the pseudo-first-order model underpredicts the concentrations; (3) the pseudo-second-order model either underpredicts or overpredicts complete ion exchange removal curves; and (4) the MS based model calculates accurate and unbiased concentrations, as the experimental data are well-distributed around the theoretical line.

Finally, it should be highlighted that the pseudo-first and pseudo-second-order equations can be used only to correlate data. The optimised constants (k_1 or k_2) cannot be applied to predict removal curves for distinct operating conditions, which severely limits their utilisation. Alternatively, our MS based model can be used with this purpose since its parameters are physical constants of fundamental transport equations, which is an obvious advantage over the two earlier expressions.

The more rigorous treatments of ion exchange processes show that no *order* can be attributed to them, i.e. no rigorous relation of the form $d\bar{q}_i/dt = f(\bar{q}_i)$ exists. The unique exception is the isotopic exchange controlled by film diffusion for which a second-order reversible rate equation is obeyed. In fact, it is impossible to provide an universal relation between the momentary rate and the average concentrations in the ion exchanger when intraparticle diffusion controls the process, since it is well-established that the momentary rate depends in this case on the shape of the non-steady concentration profiles within the sorbent and thus on the particle history [13].

5. Conclusions

In this work, the ion exchange kinetics in microporous materials were successfully modelled using a MS based model, whose parameters are the MS diffusivities of the system species and a convective mass transfer coefficient. The performance of this model was investigated with data for Cd^{2+} and Hg^{2+} removal from aqueous solutions with microporous titanosilicate ETS-4 in Na^+ form. The (AARD) achieved for the systems Cd^{2+}/Na^+/ETS-4 and Hg^{2+}/Na^+/ETS-4 were only 3.47 and 7.34%, respectively. The model calculates the concentration profiles in the exchanger phase and their evolution along time under transient regime, being able to represent the initial steep ascent branches of the removal curves and subsequent transition to the equilibrium, where kinetic curves are frequently very difficult to fit. The pseudo-first and pseudo-second-order expressions adopted for comparison provided inaccurate and significantly biased results though they are the most applied equations in the field. The average deviations were: $AARD_{Cd^{2+}} = 48.9\%$ and $AARD_{Hg^{2+}} = 26.6\%$ (pseudo-first-order), and $AARD_{Cd^{2+}} = 29.0\%$ and $AARD_{Hg^{2+}} = 54.6\%$ (pseudo-second-order).

Acknowledgements

P.F. Lito and J.P.S. Aniceto wish to thank the grants provided by Fundação para a Ciência e a Tecnologia (Portugal) (SFRH/BPD/63214/2009 and SFRH/BD/91231/2012). Authors thank Pest-C/CTM/LA0011/2011 for Associate Laboratory CICECO funding.

Nomenclature

A^{z_A}, B^{z_B}	—	counter ions with valences z_A, z_B
$\bar{A}^{z_A}, \bar{B}^{z_B}$	—	counter ions with valences z_A, z_B inside the exchanger
AARD	—	average absolute relative deviation
$[B]$	—	matrix with MS diffusivities
C_i	—	molar concentration of i in bulk solution
C_t	—	total concentration of ionic species in bulk solution
$Đ_{ij}$	—	MS diffusivity of pair $i-j$
$Đ_{is}$	—	MS diffusivity of pair i- solid
F	—	Faraday constant
k_1	—	rate constant of the pseudo-first-order equation
k_2	—	rate constant of the pseudo-second-order equation
k_f	—	convective mass transfer coefficient
K_L	—	Langmuir isotherm parameter
$[L]$	—	$= [B]^{-1}$ (see Eqs. 6 and 8)
n	—	number of counter ions
n_A	—	moles of counter ion A in solution
(N)	—	vector of molar fluxes
N_j	—	molar flux of counter ion j
q_j	—	molar concentration of counter ion j in the solid
q_{max}	—	Langmuir isotherm parameter
q_t	—	total concentration of ionic species in the solid

$\bar{q}_{A,e}$ — sorbed cation concentration at equilibrium
$\bar{q}_j$ — average concentration of j in the particle
Q — ion exchanger molar capacity
r — radial position in the particle
$\Re$ — gas constant
R — particle radius
t — time
T — absolute temperature
u_j — intraparticle velocity of j
V_L — volume of fluid phase
V_s — volume of exchanger
x_i — molar fraction of i in bulk solution
$x_{i,e}$ — molar fraction of i in solution in equilibrium with y_i
y_j — molar fraction of counter ion j in the solid
y_s — molar fraction of fixed charged groups
z_i — charge of component i

Greek letters

$\gamma_{i,eq,sol}$ — activity coefficient of counter ion i in a solution in equilibrium with particle
ϕ — electrostatic potential
$[\Gamma]$ — matrix of thermodynamic factors
Γ_{ij} — thermodynamic factors
ξ_i — related with the electrostatic potential (see Eq. 7)
μ_i — chemical potential of i
$\mu_{i,eq,sol}$ — chemical potential of i in solution in equilibrium

Subscripts

A — counter ion initially present in bulk solution (Hg^{2+} or Cd^{2+})
B — counter ion initially present in particle (Na^+)
e or eq — equilibrium
i or j — counter ion
s — solid or fixed charged groups of the particle
sol — solution
t — total

References

[1] P.F. Lito, J.P.S. Aniceto, C.M. Silva, Removal of anionic pollutants from waters and wastewaters and materials perspective for their selective sorption, Water Air Soil Pollut. 223 (2012) 6133–6155.
[2] K. Popa, C.C. Pavel, Radioactive wastewaters purification using titanosilicates materials: State of the art and perspectives, Desalination 293 (2012) 78–86.
[3] C.B. Lopes, P.F. Lito, S.P. Cardoso, E. Pereira, A.C. Duarte, C.M. Silva, Metal recovery, separation and/or concentration, in: M. Inamuddin, M. Luqman (Eds.), Chapter 11 in Ion-Exchange Technology II: Applications, Springer, London, 2012, pp. 237–322.
[4] P.F. Lito, S.P. Cardoso, J.M. Loureiro, C.M. Silva, Ion exchange equlibria and kinetics, in: M. Inamuddin, M. Luqman (Eds.), Ion-Exchange Technology I: Theory, Materials and Applications, Springer, London, 2012, pp. 51–120.
[5] J.P.S. Aniceto, S.P. Cardoso, T.L. Faria, P.F. Lito, C.M. Silva, Modeling ion exchange equilibrium: Analysis of exchanger phase non-ideality, Desalination 290 (2012) 43–53.
[6] J.P.S. Aniceto, P.F. Lito, C.M. Silva, Modeling sorbent phase nonideality for the accurate prediction of multicomponent ion exchange equilibrium with the homogeneous mass action law, J. Chem. Eng. Data 57 (2012) 1766–1778.
[7] J.P.S. Aniceto, D.L.A. Fernandes, C.M. Silva, Modeling ion exchange equilibrium of ternary systems using neural networks, Desalination 309 (2013) 267–274.
[8] D.C. Shallcross, Modelling multicomponent ion exchange equilibrium behaviour, J. Ion Exch. 14 (Supp.) (2003) 5–8.
[9] J.L. Provis, G.C. Lukey, D.C. Shallcross, Single-parameter model for binary ion-exchange equilibria, Ind. Eng. Chem. Res. 43 (2004) 7870–7879.
[10] J.L. Provis, G.C. Lukey, D.C. Shallcross, Modeling multicomponent ion exchange: Application of the single-parameter binary system model, Ind. Eng. Chem. Res. 44 (2005) 2250–2257.
[11] S. Melis, G. Cao, M. Morbidelli, A new model for the simulation of ion exchange equilibria, Ind. Eng. Chem. Res. 34 (1995) 3916–3924.
[12] A.L. Myers, S. Byington, Thermodynamics of ion exchange: Prediction of multicomponent equilibria from binary data, In: A.E. Rodrigues (Ed.), Ion Exchange: Science and Technology, Martinus Nijhoff, Dordrecht, 1986, pp. 119–145.
[13] F. Helfferich, Ion Exchange, Dover, New York, 1995.
[14] G. Kraaijeveld, J.A. Wesselingh, The kinetics of film-diffusion-limited ion-exchange, Chem. Eng. Sci. 48 (1993) 467–473.
[15] S. Edebali, E. Pehlivan, Evaluation of Amberlite IRA96 and Dowex 1×8 ion-exchange resins for the removal of Cr(VI) from aqueous solution, Chem. Eng. J. 161 (2010) 161–166.
[16] Y.S. Ho, G. McKay, The sorption of lead(II) ions on peat, Water Res. 33 (1999) 578–584.
[17] H. Faghihian, M. Kabiri-Tadi, Removal of zirconium from aqueous solution by modified clinoptilolite, J. Hazard. Mater. 178 (2010) 66–73.
[18] R. Taylor, R. Krishna, Multicomponent Mass Transfer, John Wiley, New York, 1993.
[19] G.E. Boyd, A.W. Adamson, L.S. Myers, The exchange adsorption of ions from aqueous solutions by organic zeolites. 2. Kinetics, J. Am. Chem. Soc. 69 (1947) 2836–2848.
[20] J.C.R. Turner, Nernst-planck or no, In: L. Liberty, J.R. Miller (Eds.), Fundamentals and Applications of Ion Exchange, Martinus Nijhoff, Leiden, 1985.
[21] E.E. Graham, J.S. Dranoff, Application of the Stefan-Maxwell equations to diffusion in ion-exchangers. 1. Theory, Ind. Eng. Chem. Fundam. 21 (1982) 360–365.
[22] E.E. Graham, J.S. Dranoff, Application of the Stefan-Maxwell equations to diffusion in ion-exchangers. 2. Experimental results, Ind. Eng. Chem. Fundam. 21 (1982) 365–369.
[23] J.H.G. van der Stegen, A.J. van der Veen, H. Weerdenburg, J.A. Hogendoorn, G.F. Versteeg, Application of the Maxwell-Stefan theory to the transport in ion-selective membranes used in the chloralkali electrolysis process, Chem. Eng. Sci. 54 (1999) 2501–2511.
[24] J.A. Hogendoorn, A.J.V.d. Veen, J.H.G.V.d. Stegen, J.A.M. Kuipers, G.F. Versteeg, Application of the Maxwell-Stefan theory to the membrane electrolysis process: Model development and simulation, Comput. Chem. Eng. 25 (2001) 1251–1265.
[25] G. Kraaijeveld, V. Sumberova, S. Kuindersma, H. Wesselingh, Modeling electrodialysis using the Maxwell-Stefan description, Chem. Eng. J. Biochem. Eng. J. 57 (1995) 163–176.
[26] J. Rocha, Z. Lin, Microporous mixed octahedral-pentahedral-tetrahedral framework silicates, in: G. Ferraris, S. Merlino (Eds.), Micro- and Mesoporous Mineral Phases, Washington, DC, 2005, pp. 173–201.
[27] L. Lv, K. Wang, X.S. Zhao, Effect of operating conditions on the removal of Pb^{2+} by microporous titanosilicate ETS-10 in a fixed-bed column, J. Colloid Interface Sci. 305 (2007) 218–225.

[28] J.H. Choi, S.D. Kim, Y.J. Kwon, W.J. Kim, Adsorption behaviors of ETS-10 and its variant, ETAS-10 on the removal of heavy metals, Cu^{2+}, Co^{2+}, Mn^{2+} and Zn^{2+} from a waste water, Micropor. Mesopor. Mater. 96 (2006) 157–167.
[29] E.D. Camarinha, P.F. Lito, B.M. Antunes, M. Otero, Z. Lin, J. Rocha, E. Pereira, A.C. Duarte, C.M. Silva, Cadmium(II) removal from aqueous solution using microporous titanosilicate ETS-10, Chem. Eng. J. 155 (2009) 108–114.
[30] C. Borcia, K. Popa, C.C. Pavel, A. Dascalu, C. Vitelaru, B.A. Apetrachioaei, Sorption of thallous ion from acidic aqueous solutions onto ETS-10 titanosilicate, J. Radioanal. Nucl. Chem. 288 (2011) 25–30.
[31] C.C. Pavel, K. Popa, N. Bilba, A. Cecal, D. Cozma, A. Pui, The sorption of some radiocations on microporous titanosilicate ETS-10, J. Radioanal. Nucl. Chem. 258 (2003) 243–248.
[32] C.B. Lopes, M. Otero, J. Coimbra, E. Pereira, J. Rocha, Z. Lin, A. Duarte, Removal of low concentration Hg^{2+} from natural waters by microporous and layered titanosilicates, Micropor. Mesopor. Mater. 103 (2007) 325–332.
[33] C.B. Lopes, M. Otero, Z. Lin, C.M. Silva, J. Rocha, E. Pereira, A.C. Duarte, Removal of Hg^{2+} ions from aqueous solution by ETS-4 microporous titanosilicate - kinetic and equilibrium studies, Chem. Eng. J. 151 (2009) 247–254.
[34] C.B. Lopes, M. Otero, Z. Lin, C.M. Silva, E. Pereira, J. Rocha, A.C. Duarte, Effect of pH and temperature on Hg^{2+} water decontamination using ETS-4 titanosilicate, J. Hazard. Mater. 175 (2010) 439–444.
[35] C.B. Lopes, P.F. Lito, M. Otero, Z. Lin, J. Rocha, C.M. Silva, E. Pereira, A.C. Duarte, Mercury removal with titanosilicate ETS-4: Batch experiments and modelling, Micropor. Mesopor. Mater. 115 (2008) 98–105.
[36] L.D. Barreira, P.F. Lito, B.M. Antunes, M. Otero, Z. Lin, J. Rocha, E. Pereira, A.C. Duarte, C.M. Silva, Effect of pH on cadmium (II) removal from aqueous solution using titanosilicate ETS-4, Chem. Eng. J. 155 (2009) 728–735.
[37] T.R. Ferreira, C.B. Lopes, P.F. Lito, M. Otero, Z. Lin, J. Rocha, E. Pereira, C.M. Silva, A. Duarte, Cadmium(II) removal from aqueous solution using microporous titanosilicate ETS-4, Chem. Eng. J. 147 (2009) 173–179.
[38] M. Otero, C.B. Lopes, J. Coimbra, T.R. Ferreira, C.M. Silva, Z. Lin, J. Rocha, E. Pereira, A.C. Duarte, Priority pollutants (Hg^{2+} and Cd^{2+}) removal from water by ETS-4 titanosilicate, Desalination 249 (2009) 742–747.
[39] S.P. Cardoso, C.B. Lopes, E. Pereira, A.C. Duarte, C.M. Silva, Competitive removal of Cd^{2+} and Hg^{2+} ions from water using titanosilicate ETS-4: Kinetic behaviour and selectivity, Water Air Soil Pollut. 224 (2013) 1–6.
[40] R. Krishna, J.A. Wesselingh, Review article number 50 - the Maxwell-Stefan approach to mass transfer, Chem. Eng. Sci. 52 (1997) 861–911.
[41] R. Jackson, Transport in Porous Catalysts, Elsevier, Amsterdam, 1977.
[42] W.E. Schiesser, The Numerical Method of Lines, Academic Press, San Diego, CA, 1991.
[43] S.M. Kuznicki, Preparation of Small-Pored Crystalline Titanium Molecular Sieve Zeolites, in Engelhard Corporation, 1990.
[44] N.N. Greenwood, A. Earnshaw, Chemistry of the Elements, second ed. Elsevier Butterworth Heinemann, Oxford, 2005.
[45] R.M. Barrer, L.V. Rees, Self-diffusion of alkali metal ions in analcite, Trans. Faraday Soc. 56 (1960) 709–721.
[46] N.M. Brooke, L.V.C. Rees, Kinetics of ion-exchange. 2, Trans. Faraday Soc. 65 (1969) 2728–2739.
[47] E.N. Coker, L.V.C. Rees, Ion-exchange in beryllophosphate-G.1. Ion-exchange equilibria, J. Chem. Soc.-Faraday Trans. 88 (1992) 273–276.
[48] E.N. Coker, L.V.C. Rees, Kinetics of ion exchange in quasi-crystalline aluminosilicate zeolite precursors, Micropor. Mesopor. Mater. 84 (2005) 171–178.